Research and development of effective optical technologies for diagnostics in dermatology

Vadim D. Genin*[a], Prisca Rakotomanga[c], Sergey M. Zaytsev[a,c], Elina A. Genina[a,b], Ekaterina N. Lazareva[a], Grégoire Khairallah[c], Marine Amouroux[c], Charles Soussen[c], Hang Chen[c], Wei Feng[d], Dan Zhu[d], Alexey N. Bashkatov[a,b], Walter Blondel[c], Valery V. Tuchin[a,b]
[a]Saratov State University, 83, Astrakhanskaya Str., Saratov, 410012, Russia; [b]Tomsk State University, 36, Lenina Av., Tomsk, 634050, Russia; [c]University of Lorraine, CNRS, CRAN UMR 7039, Vandoeuvre-Lès-Nancy, 54500,France; [d]Huazhong University of Science and Technology, Wuhan National Laboratory for Optoelectronics, Britton Chance Center for Biomedical Photonics, Wuhan, China

ABSTRACT

Optical Clearing (OC) of the human skin under the action of two different combinations of enhancers and OC agents was studied using two optical devices: Optical Coherent Tomography (OCT) and spatially-resolved optical spectroscopy (combining autofluorescence and diffuse reflectance spectroscopy). The *in vivo* study based onHyaluronic Acid (HA) as an enhancer for optical clearing by Polyethylene Glycol (PEG-300) was performed using OCT with the central wavelength 930 nm.The *ex vivo* study used a mixture made of sucrose, Polypropylene Glycol (PG) and PEG-400 on human skin grafts put on top of fluorescent agarose gels, resulting into an hybrid phantom model. The *in vivo* resultsshowed an increase in the transparency of the epidermis at the optical depth of 50±5 μm by 44±9 % within 15 min with the use of a solution of HA in combination with sonophoresis before application of PEG-300 to the skin surface. At the same time, when using PEG-300 without preliminary treatment of the skin with the HA, an increase in the transparency of the epidermis at the same depth was 21±8% within 25 min. In dermis at the depth of 500 μm the OCT signal in the experimental group increased more than 1.6 fold what indicates an increasing of optical probing depth. The *ex vivo* results showed that skin optical properties are modified under the action of the sucrose-PG-PEG-400 mixture after 36 min of topical application: a decrease of the scattering coefficient can be noticed. Modelling show that this may be due to a drop of water content by at least 30 %.

Keywords: human skin *in vivo*, hyaluronic acid, PEG-300, sucrose, PEG-400, PG, optical clearing, enhancer, sonophoresis, OCT, bimodal spectroscopy, modeling.

1. INTRODUCTION

The medical context of our works is the one of *in vivo* noninvasive photodiagnosis of skin carcinoma. Skin cancers initiate in the epidermis before spreading deepward throughout the dermis. Indeed precancerous and cancerous evolution of skin results in modifications in its structure, organization, composition and metabolism, at cellular and tissular levels.[1,2] And these modifications change the optical properties (OP) of the skin. Thus, our research works focus on the *in vivo* characterization of skin OPusing optical biopsy based approaches and their translation into clinics in order to improve medical diagnosis performance. To increase detection sensitivity and specificity and to probe the tissue at various depths, our developments are focused on fibered spectroscopy tools exploiting (i) multimodality by collecting Diffuse Reflectance (DR) and multiply excited AutoFluorescence (AF) emission spectra and (ii) spatially-resolved measurements through a multifiber probe.[3,4]

In order to estimate the values of *in vivo* tissue OP, an optical model of skin has to be considered including absorption, scattering and fluorescence features. The values of these model parameters have to be estimated by solving the corresponding inverse problem. Skin is characterized by strong absorption namely due to melanin in the epidermis and hemoglobin in the dermis, and by high scattering due to the stack of cell layers and variety of tissue constituents that are so many optical interfaces. This is the reason why changing the skin transparency may help to probe more efficiently the

*versetty2005@yandex.ru

Saratov Fall Meeting 2018: Optical and Nano-Technologies for Biology and Medicine, edited by Elina A. Genina, Valery V. Tuchin, Proc. of SPIE Vol. 11065, 1106505 · © 2019 SPIE
CCC code: 0277-786X/19/$18 · doi: 10.1117/12.2528700

various skin layers and contribute to an improved medical diagnosis.[5-8] Therefore, safe Optical Clearing Agents (OCAs) need to be investigated.

Nowadays the interest in the use of OCAs constantly increases. The OCAs make it possible to increase the probing depth of noninvasive optical diagnostic methods including fluorescent ones, they are biocompatible[9], safe and inexpensive.[10,11] Polyethylene glycols (PEGs) are immersion liquids that are widely used as OCAs, due to their effectiveness, availability and biocompatibility.[12,13] However, the protective epidermal barrier of the skin prevents the penetration of hydrophilic immersion liquids into the deeper layers of the skin. For enhancement of stratum corneum permeability for hydrophilic OCAs different chemical agents and physical methods are used.

Hyaluronic acid (HA) is a non-sulfated glycosaminoglycan that is a part of the connective, epithelial and nervous tissues. It is one of the main components of the interstitial matrix, found in many natural lubricating biological fluids (saliva, synovial fluid, etc.).[14] The action of HA as a skin moisturizer is based on the ability of this substance to bind moisture (a 2% aqueous solution of pure HA retains the remaining 98% of water, forming a gel).[15] It was shown that HA can enhance the skin permeability for immersion agents.[16,17] However, these studies were performed *in vitro* with skin samples of minipigs. In this cases, the HA was applied on the dermis side directly.[17]

The use of ultrasound (US) with a frequency of 1-1.5 MHz (sonophoresis) as a physical permeation enhancer allows for deeper introduction of OCAs.[18-20] The US-induced cavitation provides formation of microbubbles in skin. As a result, internal cavities passing through the stratum corneum are created as well as the damage and disturbance of the cell ordering that lead to the loosening of epidermal layer.[19,21]

The present contribution is a combined study of the efficiency of optical clearing of human skin (i) *in vivo* with increasing permeability of the epidermis for PEG-300 thanks to the combined use of Hyaluronic Acid (HA) solution and sonophoresis, observed using Optical Coherence Tomography (OCT) and (ii) *ex vivo* through the modifications of skin OP estimated from spatially resolved DR and AF spectroscopy.

2. MATERIALS AND METHODS

2.1. Optical Coherence Tomography

For the skin optical clearing, PEG-300 (*Sigma-Aldrich*, USA) was used. As an enhancer for epidermis permeability the water solution of HA (*Evalar*, Russia) with concentration 36 mg/mL was used. The refractive indices of PEG-300 and HA measured by multi-wavelength refractometer *DR-M2/1550* (*ATAGO*, Japan) at the wavelength 930 nm were 1.456 and 1.325, respectively.

The sonophoresis with an US-device *Dynatronics 125* (*Dynatrone*, USA) with 2 cm diameter probe in CW mode (with frequency 1 MHz and power density 1 W/cm^2) was applied.

The *in vivo* experiment included investigation of six human skin areas on the back of the forearms of the two volunteers 20-25 years old. The study was approved by the Ethics Committee of the Saratov State Medical University.

Three skin areas were included in the experimental group, another three were included in the control group. Before experiment skin areas were treated with 40% alcohol solution. Then a solution of HA was applied to the skin areas of the experimental group, and within 1 min the skin surface was sonificated. Thereafter PEG-300 was applied to the skin areas, and also sonificated for 2 min. In the control group HA was not applied.

Optical coherence tomography was used for skin monitoring before the treatments and every 5 min after PEG-300 application using a spectral OCT system *Thorlabs OCP930SR* (*Thorlabs*, USA) with the following parameters: central wavelength of 930±5 nm, axial and lateral resolution of 6.2 μm and 9.6 μm respectively (in air), the length of the scanning area of 2 mm.

2.2. Spatially resolved Diffuse Reflectance (DR) andAutoFluorescence (AF) spectroscopy

A fibered-optical spectroscopy device developed for clinical application was used to acquire DR spectra in the wavelength range 350-800 nm and AF spectra excited at five wavelength peaks λ_{exc} = 365, 385, 395, 405 and 415 nm respectively.[22] The multiple optical fiber probe is made of one central excitation fiber (600 μm in diameter) surrounded by three rings of six collecting fibers each (200 μm in diameter) organized at three distances from the center fiber *i.e.* D1 = 400 μm, D2 = 600 μm and D3 = 800 μm.

Measurements were performed on a skin-gel bilayer experimental model made of (i)on top (upper layer), a 440 µm thick *ex vivo* skin strip harvested using a dermatome on human skin wastes and (ii) a bottom consisting in a 5 mm-thick agarose gel with NanoParticles (NP) of Terbium and porphyrin (Tb@P_1) allowing high hydro-solubility of the latter in agarose.Skin wastes were used after authorization was given by fully-informed patients undergoing surgery and after the Ethics Evaluation Committee of INSERM (IRB00003888)approved the protocol (authorization # 17-400). The main fluorescence excitation wavelength peak of Tb@P_1 is around 420 nm with emission peaks at 655 and 720 nm. OCA and enhancer consisted of a mixture of 50 % 3M-sucrose, 45 % Polyethylene Glycol PEG-400 and 5 % Polypropylene Glycol (PG). Three milliliters (3 mL) of this OCA solution were applied on top of the skin sample during 12, 24 and 36 min total.Spectroscopic measurements were started at T_0 (skin without OCA) then iterated every 12 min at T_0+12, T_0+24 and T_0+36 min, respectively.

A 4-layer model was implemented for our skin strip, based on works of Petrov*et al.*[23] It takes into account the absorption coefficients of eumelanin$\mu_a^{eu}(\lambda)$, pheomelanin$\mu_a^{phe}(\lambda)$, hemoglobin and water$\mu_a^{H_2O}(\lambda)$ and their relative volume fractions B_{mel}, C_{mel}, Kb,S, C_{H_2O}in the different layers considered here Stratum Corneum (SC), Living Epidermis (LE), Papillary Dermis (PD) and Reticular Dermis (RD) defined as follows:

$$\mu_a^{SC}(\lambda) = \left(1 - c_{H_2O}\right) \times \mu_a^{base}(\lambda) + c_{H_2O} \times \mu_a^{H_2O}(\lambda)$$

$$\mu_a^{LP}(\lambda) = \left(1 - c_{H_2O}\right)\left[C_{mel} \times \left(B_{mel} \times \mu_a^{eu}(\lambda) + (1 - B_{mel}) \times \mu_a^{phe}(\lambda)\right) + (1 - C_{mel}) \times \mu_a^{base}(\lambda)\right] + C_{H_2O} \times \mu_a^{H_2O}(\lambda)$$

$$\mu_a^{PD/RD}(\lambda) = \left(1 - c_{H_2O}\right)\left[Kb \times \left(S \times \mu_a^{HbO_2}(\lambda) + (1 - S) \times \mu_a^{Hb}(\lambda)\right) + (1 - Kb) \times \mu_a^{base.}(\lambda)\right] + C_{H_2O} \times \mu_a^{H_2O}(\lambda)$$

The analytical expression of the scattering coefficient for each layer combines Rayleigh and Mie scattering such as:

$$\mu_s(\lambda) = N \times (2{,}2 \times 10^{12} \times \lambda^{-4} + 117.4 \times \lambda^{-0{,}22})$$

The spectral curves of the various absorption coefficients being *a priori* defined, the parameters to be estimated are the volume fraction coefficients B_{mel}, C_{mel}, Kb, S, C_{H_2O} and N.Finally, the optical properties of the bottom gel layer include fluorescence absorption and emission parameters related to the NP.

Our estimation scheme is based on the least square cost function $f(p;\lambda,D)$ expressed hereafter between experimental DR spectra $R_{exp}$and simulated ones R_{mod} as a function of the wavelentghs λ_i, of the interfiber distances D_j and of the parameter vector p. A modified cuda MCML code running on GPU card was implemented and included fluorescence as well. This cost-function was minimized so as to obtain optimized values for the p vector through a Trust Reflective Region algorithm together with a random drawing of ten (10) starting points around *a priori* values of the parameters taken from the literature.

$$f(p;\lambda,D) = \sum_{i}^{N_\lambda}\sum_{j}^{N_D}\left[R_{exp}(\lambda_i,D_j) - k(D_j)R_{mod}(p;\lambda_i,D_j)\right]^2$$

3. RESULTS AND DISCUSSION

3.1. OCT

In Figure 1 the typical OCT B-scans of the skin areas from experimental and control groups at the different moments of experiment are presented. It can be seen that the clearing of the skin after pre-application by the HA is more effective: the lightened area in the B-scans in the experimental group is larger than in the control one.

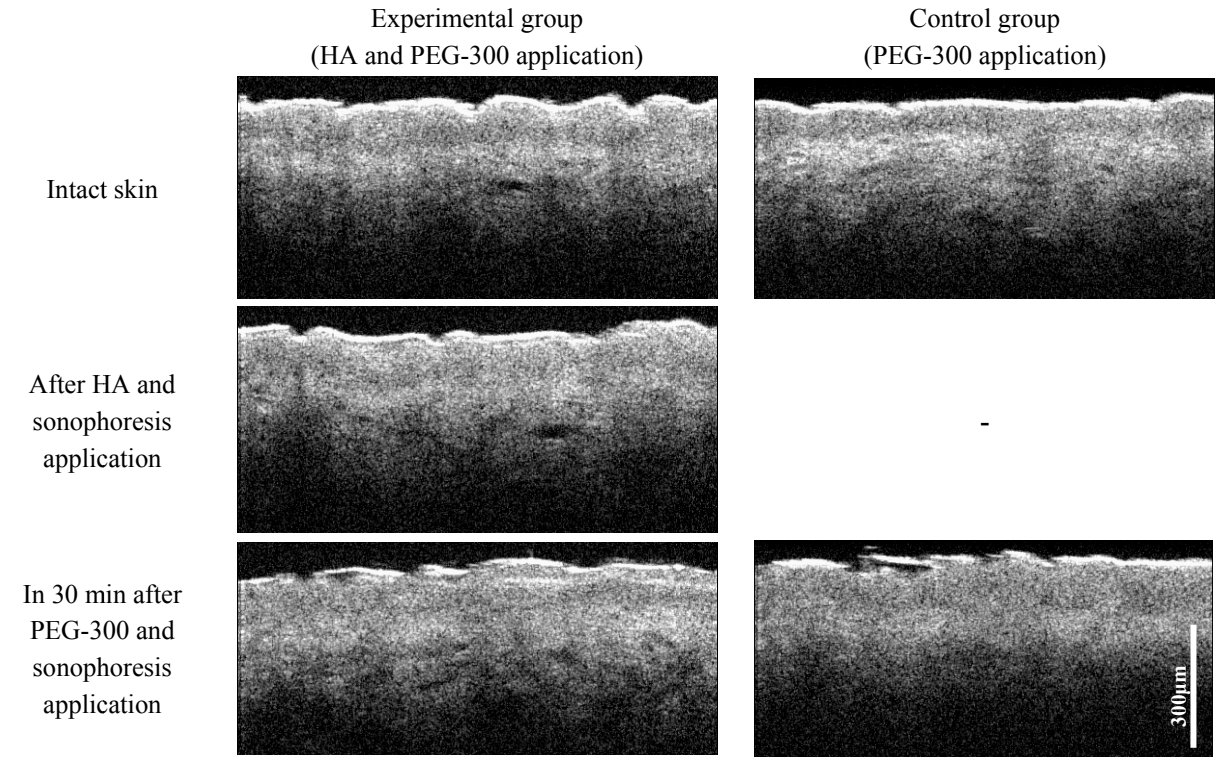

Figure 1. The typical OCT scans of the skin areas from experimental and control groups at the different stages of experiment

To evaluate the kinetics of OCT-signal in the both epidermis and dermis after different treatments, the noise signal was subtracted from the informative signal, and the obtained values were normalized on the signal from intact skin. Figure 2 shows the kinetics of the OCT signal in the epidermis (50±5 μm) and at theoptical depth of 500±5 μm, averaged over all samples and normalized to an initial value corresponding to the OCT signal from intact skin.

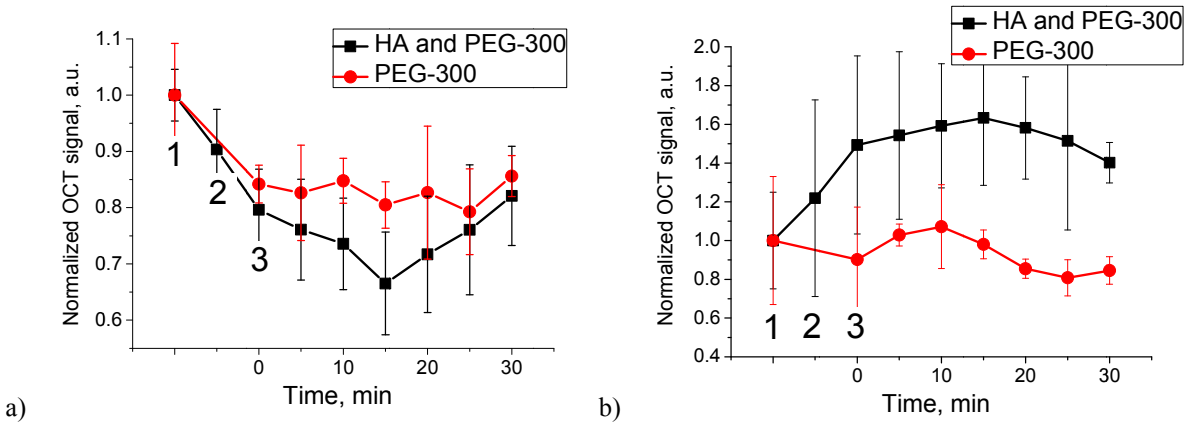

Figure 2. The kinetics of the OCT signal at the optical depths of the skin of 50±5 μm (a) and 500±5 μm (b), averaged over all samples and normalized to the initial value corresponding to the OCT signal from intact skin. The numbers indicate the points in time corresponding to the registration of the signal from the intact skin (1); after the application of HA and sonophoresis (2) and after the application of PEG-300 and sonophoresis (3).

In Figure 2 it can be seen that optical clearing led to the decrease in the OCT signal in the epidermis by 44±9% (in 15 min). In the control group, the maximum skin clearing was achieved for a longer time (25 min) and the decrease of the OCT signal was 21±8%. At the optical depth of 500±5 μm, the signal for the control group practically did not change with time (the changes were not statistically significant), while in the experimental group it increased on average by

more than 1.6 fold. We believe that during the measurements, the investigated agents did not penetrate into the dermis to a depth of 500 µm, therefore, an increase in the probing depth occurred mainly due to the increase in the transparency of the epidermis and upper layers of dermis.

3.2. Spatially resolved DR and AF spectroscopy

Results in terms of DR spectra are presented in Figure 3 (first row) at T_0 (before OCA application on skin) and at T_0+36 after maximum duration of OCA application. It can be observed an overall decrease in amplitude with OCA application (a factor of more than 2 for spectra collected at D1) except at longest wavelengths and longest distances (for instance 20% more signal is collected at D2 at 655nm that is related to the fluorescence emitted from the gel layer). Indeed, much less photons collected at D1 and more photons collected at D2 and D3 at longest wavelength are in favor of strong decrease in absorption and scattering properties of skin. In spite of differences in fiber opticalprobe construction with the source-detector separations of 1.14, 2.08, and 3.5 mm, DR behavior found in this paper is well fit to that discovered for *in vivo* human skin studies on the wavelength 786 nm[24], with monotonic decay for small interfiber distances and nonmonotonic behavior (first growing and then decay) with time at topical application of glycerol during 20 min.

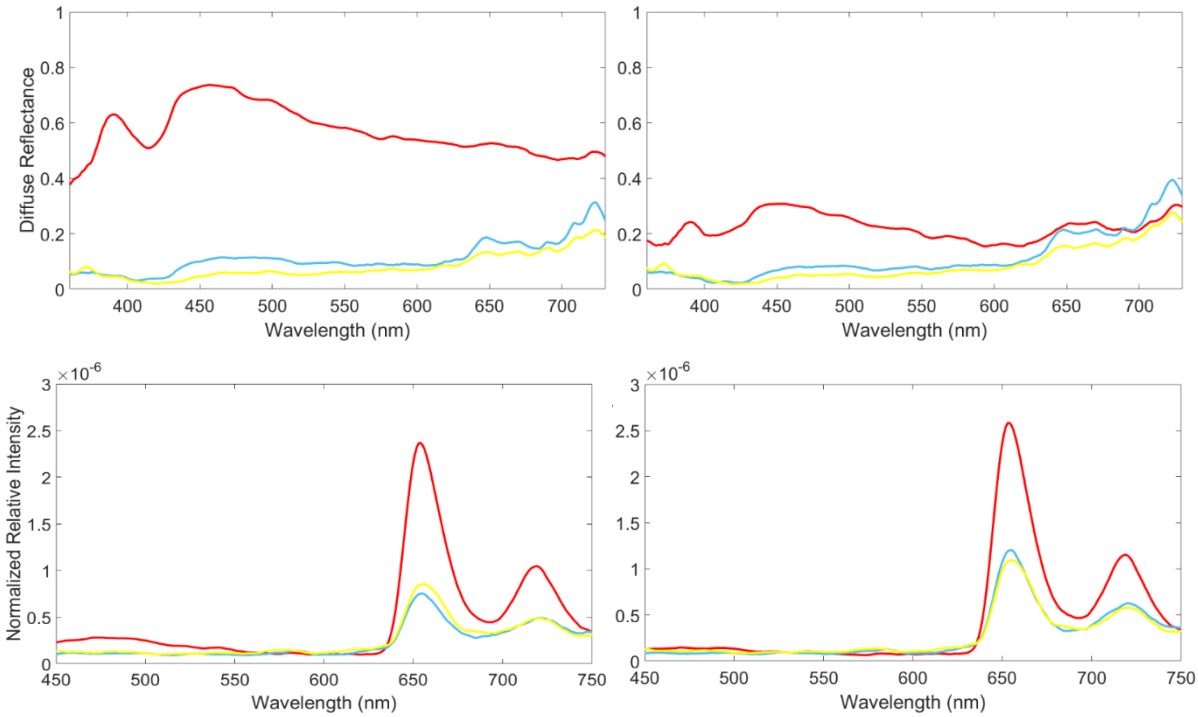

Figure 3. DR (first row) and 405 nm excited fluorescence (second row) spectra at T_0 before OCA application (left) and at T_0+36 after 36 min application (right). Interfiber distances D1 = 400 µm, D2 = 600 µm and D3 = 800 µm are in red, blue and yellow colors, respectively.

Looking at fluorescence intensity spectra excited at 415 nm shown in Figure 3 (second row), at T_0, it can be observed skin AF emission with a peak around 475 nm and bottom gel P1 fluorescence with emission peaks at 655 and 720 nm. At T_0+36, the amplitude of skin AF signal is decreased by a 2.35 factor while bottom layer fluorescence amplitude displays a 20 to 60% increase at longest distances D2 and D3. Here again our interpretation is that less skin AF photons (coming from top layer i.e. skin) were collected at D1 while more bottom layer fluorescence photons were collected at D2 and D3, which is again in favor of strong decrease in absorption and scattering properties of skin after OCA application.

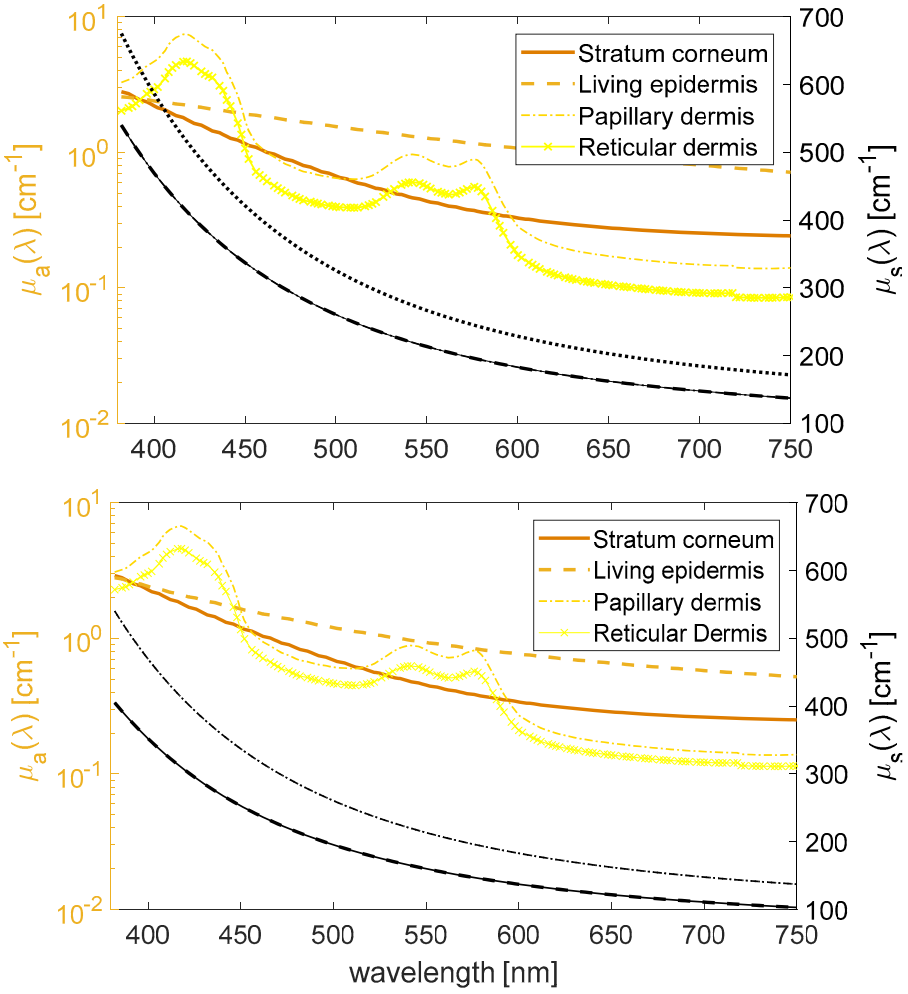

Figure 4. Estimated spectra of absorption (left vertical scale, yellow and brown color curves) and scattering (right vertical scale, black curves) coefficients $\mu_a^{SC}(\lambda)$, $\mu_a^{LP}(\lambda)$, $\mu_a^{PD}(\lambda)$, $\mu_a^{RD}(\lambda)$, $\mu_s(\lambda)$at T_0 before OCA application (top) and at T_0+36 after 36 min application (bottom).

The estimated values of the OP of our 4-layer model are plotted in Figure 4. They were based on a selection of 17 wavelength values over the 350-750 nm spectral range. The left vertical axis refers to $\mu_a(\lambda)$ values with 4 yellow and orange curves correspond to the 4 layers of our skin model while the right vertical axis refers to$\mu_s(\lambda)$ spectra in black. Both are in cm^{-1} units. For the SC layer, although $\mu_a^{SC}(\lambda)$values are close, a 3 fold-decrease can be noticed for the water volume fraction ($C_{H_2O} = 0.05$ and 0.017 at T_0 and T_0+36, respectively), and by a factor of 1.3 for $\mu_s(\lambda)$ with parameter $N = 4$ at T_0 and $N = 3$ at T_0+36. For the LE layer, estimated values of the volume fractions of water and melanin showed a decrease by a factor of 2.2 and 2 respectively with $C_{H_2O} = 0.2/0.017$ and $C_{mel} = 0.1/0.05$ at T_0 / T_0+36, respectively. $\mu_s(\lambda)$ values for LE layer were identical to the SC layer ones. For the PD layer, a decrease by a factor of 1.5 can be noticed for both the water volume fraction and the blood fraction coefficient (including RBC, hemoglobin and hematocrit) with $C_{H_2O} = 0.5/0.33$ and $Kb = 0.0045/0.003$ at T_0 / T_0+36, respectively. A decrease factor of 1.3 was also obtained for $\mu_s(\lambda)$. Concerning the RD layer, a higher decrease is obtained for water volume fraction ($C_{H_2O} = 0.7$ and 0.33 at T_0 and T_0+36, respectively) and a lower one for the blood volume fraction coefficient($Kb = 0.0045/0.0037$ at T_0/T_0+36, respectively). It is finally to be noticed that $\mu_s(\lambda)$ seems to be little or no modified in this layer.

4. CONCLUSION

The results of the study have shown the decrease of the OCT signal from the epidermis at a depth of 50 μm by 44±9% for 15 min when using the combination of HA solution with sonophoresis and PEG-300 on the skin surface, which indicates the increase in the transparency of the epidermis. In the dermis, the OCT signal has increased by more than 1.6 fold, which indicates the increase of the OCT probing depth in skin. At the same time, when using PEG-300 without pre-treatment of the skin with HA, the decrease of the OCT signal in the epidermis within 25 min was 21±8%. At the optical depth of about 500 μm, the signal has remained almost unchanged.

The modifications of the estimated OP of an *ex vivo* skin strip induced by topical application of OCA are clearly assessed on spatially resolved DR and fluorescence spectra with less upper layer skin DR photons collected and more bottom gel P1 fluorescence photons collected at longer interfiber distances. The corresponding variations in $\mu_a(\lambda)$ and $\mu_s(\lambda)$ are confirmed by their numerical estimation with 30 to 60% decrease in water volume fraction and 25% decrease in scattering coefficient. This preliminary study confirms the interest of combining depth sensitivity of SR-bimodal spectroscopy and OCA in order to provide additional information about *in vivo* tissue depth profile that may be of clinical interest for skin cancers surgical management.

ACKNOWLEDGEMENTS

The study was supported by the RFBR grant 18-52-16025, the Vernadski Grant from the French Embassy in Moscow (supporting the French-Russian co-supervised PhD student Sergey Zaytsev), the French Emabassy in China (Xu Guangqi 2018), the French-Chinese International Research Network IRN *Photonet*, the CRAN laboratory internal support (*actions incitatives*) for international cooperation, the Clinical trial award by the Metz-Thionville Regional Hospital (CHR Metz-Thionville) and the CPER 2015-2020 (FEDER, Grand Est Region, LigueContre le Cancer and the French Ministry of Research and Innovation).

REFERENCES

[1] Yudovsky D., L. Pilon, "Rapid and accurate estimation of blood saturation, melanin content, and epidermis thickness from spectral diffuse reflectance." App. Optics, 49, 1708-1719 (2010).
[2] Kollias N., Zonios G., Stamatas G.N., "Fluorescence spectroscopy of skin," Vib. Spectro., 28, 17-23 (2002).
[3] Amouroux M., Díaz-Ayil G., Blondel W., "Classification of ultraviolet irradiated mouse skin histological stages by bimodal spectroscopy: multiple excitation autofluorescence and diffuse reflectance." J. Biomed. Optics, 14(1), 1-14 (2009).
[4] Abdat F., Amouroux M., Guermeur Y., Blondel W. "Hybrid feature selection and SVM-based classification for mouse skin precancerous stages diagnosis from bimodal spectroscopy." Opt. Exp., 20(1), 228-244 (2012).
[5] Sdobnov A.Y., Darvin M.E., Genina E.A., Bashkatov A.N., Lademann J., Tuchin V.V., "Recent progress in tissue optical clearing for spectroscopic application." Spectrochimica Acta Part A: Mol. and Biomol. Spectr., 197, 216-229 (2018).
[6] Pires L., Demidov V., Vitkin I.A., Bagnato V., Kurachi C., Wilson B.C., "Optical clearing of melanoma *in vivo*: characterization by diffuse reflectance spectroscopy and optical coherence tomography." J. Biomed. Optics, 21(8), 1-9 (2016).
[7] Vargas G., Chan K.F., Thomsen S.L., Welch A.J., "Use of osmotically active agents to alter optical properties of tissue: Effects on the detected fluorescence," Lasers Surg. Med., 29, 213- 220 (2001).
[8] Migacheva E.V., Pravdin A.B., Tuchin V.V., "Alterations in autofluorescence signal from rat skin ex vivo under optical immersion clearing," J. Innov. Opt. Health Sc., 3, 147-152 (2010).
[9] Tuchin V.V., "Optical clearing of tissues and blood using the immersion method" J. Phys. D: Applied Physics 38, 2497-2518 (2005).
[10] Genina E.A., Bashkatov A.N., Tuchin V.V., "Tissue optical immersion clearing" Expert Review of Medical Devices 7(6), 825-842 (2010).
[11] Zhu D., Larin K., Luo Q., Tuchin V.V., "Recent progress in tissue optical clearing" Laser & Photonics Reviews 7(5), 732-757 (2013).

[12] Zhi Z., Han Z., Luo Q., Zhu D., "Improve optical clearing of skin in vitro with propylene glycol as a penetration enhancer" J.Innov. Opt. Health Sci. 2(3), 269-278 (2009).
[13] Wang J., Zhang Y., Xu T.H., Luo Q.M., Zhu D., "An innovative transparent cranial window based on skull optical clearing" Laser Physics Letters 9(6), 469-473 (2012).
[14] Stern R., "Hyaluronan catabolism: a new metabolic pathway" Eur. J. Cell Biol. 83 (7), 317-25 (2004).
[15] Paye M., Barel A.O., Maibach H.I. (Eds.), [Handbook of cosmetic science and technology], Taylor and Francis Publ, Boca Raton, FL, USA (2006).
[16] Lee S.G., Jeong J.H., Lee K.M., Jeong K.H., Yang H., Kim M., Jung H., Lee S., Choi Y.W., "Nanostructured lipid carrier-loaded hyaluronic acid microneedles for controlled dermal delivery of a lipophilic molecule" Int. J. Nanomed. 9, 289-299 (2014).
[17] Liopo A., Su R., Tsyboulski D.A., Oraevsky A.A., "Optical clearing of skin enhanced with hyaluronic acid for increased contrast of optoacoustic imaging" J. Biomed. Opt. 21(8), 081208 (2016).
[18] Genina E. A., Bashkatov A.N., Kolesnikova E.A., Basko M.V., Terentyuk G.S., Tuchin V.V. "Optical coherence tomography monitoring of enhanced skin optical clearing in rats in vivo" J. Biomed. Opt. 19(2) 021109 (2014).
[19] Xu X., Sun C. “Ultrasound enhanced skin optical clearing: microstructural changes,” J. Innov. Opt. Health Sci. **3**(3), 189-194 (2010).
[20] Zhong H., Guo Z., Wei H., Guo L., Wang C., He Y., Xiong H., Liu S. "Synergistic effect of ultrasound and Thiazone- PEG 400 on human skin optical clearing *in vivo*" Photochem. Photobiol. 86, 732-737 (2010).
[21] Lavon I., Grossman N., Kost J., Kimmel E., Enden G. “Bubble growth within the skin by rectified diffusion might play a significant role in sonophoresis” J. Controlled Release 117(2), 246–255 (2007).
[22] Amouroux M., Blondel W., Delconte A. “Medical device for fibred bimodal optical spectroscopy”. WO2017093316A1(2015).
[23] Petrov G.I., Doronin A., Whelan H.T., Meglinski I., Yakovlev V.V.“Human tissue color as viewed in high dynamic range optical spectral transmission measurements.” Biomed. Opt. Exp., 3(9), 2154-2161 (2012).
[24] Tuchin V.V., Culver J., Cheung C., Tatarkova S.A., Della Vecchia M.A., Zimnyakov D., Chaussky A., Yodh A.G., Chance B. “Refractive Index Matching of Tissue Components as a New Technology for Correlation and Diffusing-Photon Spectroscopy and Imaging,” Proc. SPIE 3598,111-120 (1999).